Macroscopic network circulation for planar graphs

Fariba Ariaei*, Zahra Askarzadeh*, Yongxin Chen and Tryphon T. Georgiou

***Abstract*— The analysis of networks, aimed at suitably defined functionality, often focuses on partitions into subnetworks that capture desired features. Chief among the relevant concepts is a *2-partition*, that underlies the classical Cheeger inequality, and highlights a constriction (bottleneck) that limits accessibility between the respective parts of the network. In a similar spirit, the purpose of the present work is to introduce a concept of *macroscopic circulation* and to explore *3-partitions* that expose this type of feature in flows on networks. It is motivated by transportation networks and probabilistic flows (Markov chains) on graphs. While we introduce and propose such notions in a general setting, we only work out the case of planar graphs. Specifically, we explain that circulation depends on a scalar potential in a manner that is similar to the curl of planar vector fields. For general graphs, assessing global circulation remains at present a combinatorial problem.**

I. Introduction

Time asymmetry of traffic flow in city streets is unmistakeable. Specifically, traffic flows in one direction around city squares and, often, in one-way in many city streets as well. Yet, from a macroscopic vantage point, circulation may or may not be evident. Flux from one part of town to another may average out with flux in the opposite direction. When this is not the case, it is of interest to identify the nature and to quantify any large scale flow imbalance. What we seek in the present article is precisely such a notion of *macroscopic circulation* that, depending on the network and flow conditions, captures the flow asymmetry and a preference in directionality while traversing the graph.

Perhaps, circulation is nowhere more apparent than in air currents at the planetary scale. The vorticity, locally as well as at earth-scale, very much as in planar vector fields, can be quantified by a suitably defined scalar potential. In turn, as we will explain, this scalar potential helps quantify maximal circulation macroscopically.

Supported in part by the NSF under grants 1807664, 1839441, 1901599, and the AFOSR under FA9550-17-1-0435.

F. Ariaei, Z. Askarzadeh, and T. T. Georgiou are with the Department of Mechanical and Aerospace Engineering, University of California, Irvine, CA; rfu2@uci.edu, ataghvae@uci.edu, tryphon@uci.edu

Y. Chen is with the School of Aerospace Engineering, Georgia Institute of Technology, Atlanta, GA 30332; yongchen@gatech.edu

*F. Ariaei and Z. Askarzadeh contributed equally to this work as first authors.

In this work we define a notion of macroscopic circulation for graphs. At present, computing macroscopic circulation in general is a combinatorial problem. For the special case of embedded planar graphs, taking advantage of insights from the Helmholtz-Hodge decomposition of vector fields, we explain on how circulation can be effectively computed by determining a scalar potential with support on the nodes of the dual graph.

We contemplate a setting where a stationary discrete-time Markov model models probability flux on the network of the nodes and edges of the Markov chain. In this setting, the famous Cheeger inequality relates the likelihood of transitioning between two parts in a 2-partition of the nodes as well as the rate of mixing, to spectral properties of the graph Laplacian; the 2-partition captures bottlenecks that impede mixing.

In a similar manner, considering circulatory imbalance, we are led to a 3-partition of a network; in a 2-partition stationary probability currents across the boundary balance out. Circulatory asymmetry can only manifest when more than two components exchange "mass." For a 3-state partitioning of a network into parts A, B, and C, the net flow from A $\to$ B (considered positive when the net flux is in the direction of B), by mass conservation, must equal to the net flux from B $\to$ C, and must also equal the net flux from C $\to$ A. The asymmetry manifests itself as a network circulation current. For reasons akin to those underlying the Cheeger constant, careful consideration of the size and regularity of the boundary between parts is warranted.

The structure of the paper is as follows. In Section II, we discuss probability currents and flow fields on graphs. In Section III, we highlight the concept of macroscopic circulation for Markov chains. The setting of Markov chains is not restricted by the dimensionality of possible embedding of the respective graph, but the formulation of circulation in general requires further refinement. In Section IV, we discuss planar graph. In section V, we explain how to calculate the scalar potential supported on the dual graph and a method for partitioning the graph into three parts for assessing macroscopic circulation. The issue of embedding is revisited in Section VI where it is explained that a given graph may have non-equivalent embeddings, leading to

different values for the macroscopic circulation.

II. Currents & flow fields on graphs

We explain flows on graphs and probability currents, induced by a Markov structure.

Consider a time-homogeneous, discrete-time, N-state finite Markov chain X_t, with $t \in \mathbb{N}$, with states $\mathcal{V} = \{v_1, \dots, v_N\}$, comprised of the nodes of a network, and transition probabilities π_{v_i,v_j}, i.e.,

$$\mathbb{P}\{X_{t+1} = v_j \mid X_t = v_i\} = \pi_{v_i,v_j}.$$

We assume that the Markov chain is ergodic and hence, irreducible and aperiodic. Thus, the matrix $\Pi := [\Pi_{v_i,v_j}]_{v_i,v_j=1}^N$ has non-negative entries and is such that $\Pi\mathbf{1} = \mathbf{1}$, where $\mathbf{1}$ denotes a column vector with all entries equal to 1. The ergodicity assumption implies that for a sufficiently large integer k (e.g., $k = N$), Π^k has all entries positive. The dimensionality of vectors and matrices will be explicit, unless their dimension is clear from the context.

The Markov chain is associated to a graph $\mathcal{G} := (\mathcal{V}, \mathcal{E})$, where the (directed) edge set $\mathcal{E}$ is specified by the allowed transitions, i.e.,

$$\mathcal{E} = \{e = (v_i, v_j) \,|\, \pi_{v_i,v_j} \neq 0\}.$$

We consider $\mathcal{G}$ to have only one edge for any ordered pair of nodes. Further, $\mathcal{G}$ is strongly connected due to the ergodicity assumption.

Let now $\pi = [\pi_{v_i}]_{v_i=1}^N$ denote the (column) stationary probability vector of the Markov chain. Thus,

$$\pi^T \Pi = \pi^T$$

and π^T is the (unique left/row Frobenious-Perron) eigenvector of Π with eigenvalue 1. Throughout, ^{T} denotes transposition. The entries of

$$P := \mathrm{diag}(\pi_{v_1}, \dots, \pi_{v_N})\Pi \tag{1}$$

represent probability current $p_{v_i,v_j} = \pi_{v_i}\pi_{v_i,v_j}$ from vertex/state v_i to v_j. Probability currents quantify *flux* on $\mathcal{G}$.

Our aim is to identify (large scale) imbalance in the *net flux* across $\mathcal{G}$, and to this end, we will be working with the antisymmetric part of P (modulo a factor of $1/2$)

$$F = P - P^T. \tag{2}$$

This retains information on only local flux imbalance between nodes. Note that since, $\Pi\mathbf{1} = \mathbf{1}$ and $\pi^T\Pi = \pi^T$, it follows that $P\mathbf{1} = P^T\mathbf{1}$, and therefore, that $F\mathbf{1} = \mathbf{0}$ (the zero vector) as well.

We view the matrix F as representing a "divergence free" (i.e., with no sources) *flow ("vector") field* on $\mathcal{G}$. Besides the fact that

$$F = -F^T \tag{3a}$$

$$F\mathbf{1} = \mathbf{0}, \tag{3b}$$

the positive part of F, namely,

$$F_+ := [\max\{F_{ij}, 0\}]_{i,j=1}^n,$$

has entries that are less than or equal to P, and since $\mathbf{1}^T P\mathbf{1} = 1$,

$$\mathbf{1}^T F_+ \mathbf{1} \leqslant 1. \tag{3c}$$

It turns out that (3a-3c) characterize divergence-free flow fields on graphs, i.e., *antisymmetric matrices satisfying (3b-3c) originate from a Markovian probability structure*, as stated next

Proposition 1. *Let F be and $n \times n$ matrix satisfying (3a-3c). In case* (3c) *holds with equality, assume that $\mathbf{1}^T F_+$ has all entries positive. Then, F originates as a divergence-free flow-field on a graph $\mathcal{G} = (\mathcal{V}, \mathcal{E})$, with $|\mathcal{V}| = n$, associated with a Markov chain.*

Proof. If (3c) holds with equality, let $P = F_+$, otherwise define $P := M + F_+$, for a symmetric matrix $M = M^T$, of the same size, with nonnegative entries such that

$$\mathbf{1}^T M\mathbf{1} = 1 - \mathbf{1}^T F_+ \mathbf{1},$$

ensuring that $\pi^T := \mathbf{1}^T P$ has all entries positive. This is clearly possible from the standing assumptions. Now, verify that

$$\Pi = \mathrm{diag}(\pi_{v_1}, \dots, \pi_{v_N})^{-1} P \tag{4}$$

is a transition probability matrix that leads to the divergence-free flow field F. Specifically, i) Π has non-negative entries. ii) In view of $\pi^T = \mathbf{1}^T P$ and (4), $\pi^T\Pi = \pi^T$ holds. iii) Note that $F = F_+ - F_+^T$ and hence, $F_+\mathbf{1} = F_+^T\mathbf{1}$ from (3b). It follows that $P\mathbf{1} = P^T\mathbf{1}$, and from (4) the definition $\pi^T = \mathbf{1}^T P$, that $\Pi\mathbf{1} = \mathbf{1}$. iv) Lastly, $P - P^T = F_+ - F_+^T = F$. □

III. Macroscopic circulation on graphs

Consider an $N \times N$ antisymmetric matrix F of net fluxes that defines a divergence-free[1] flow field on a (simple) graph $\mathcal{G}$. We seek a suitable definition of (maximal) *macroscopic circulation* by partitioning the states into three subsets A, B, and C, in such a way so as to maximize the flux between the parts.

[1]If this is not the case, we replace F by its restriction on the complement of the range of $\mathbf{1}\mathbf{1}^T$, namely, $(I - \frac{1}{n}\mathbf{1}\mathbf{1}^T)F(I - \frac{1}{n}\mathbf{1}\mathbf{1}^T)$, so that $F\mathbf{1} = 0$.

For the case of a three-state Markov chain ($\mathsf{N} = 3$), the net flux matrix (antisymmetric part of the probability current matrix P, modulo a factor of $1/2$) is

$$\mathsf{F} = \begin{bmatrix} 0 & -\gamma & \gamma \\ \gamma & 0 & -\gamma \\ -\gamma & \gamma & 0 \end{bmatrix},$$

with the directionality encoded in the sign of γ. Obviously, the off-diagonal entries of F must have the same magnitude, since $\mathsf{F}\mathbf{1} = 0$. Evidently, the value $|\gamma|$ quantifies circulation in this example.

In the general case with N states, we seek partitioning the graph into three subsets of nodes

$$\mathcal{A}, \mathcal{B}, \mathcal{C} \subset \mathcal{V}$$

that are pairwise non-intersecting with

$$\mathcal{V} = \mathcal{A} \cup \mathcal{B} \cup \mathcal{C}.$$

Such a triple of subsets of $\mathcal{V}$ will be referred to as a 3-partition.

Define the characteristic (column) vector $\mathrm{I}_{\mathcal{S}}$ of a set $\mathcal{S} \subseteq \mathcal{V}$, with $\mathcal{V}$ ordered, as follows: the ν^{th} entry of $\mathrm{I}_{\mathcal{S}}$ is equal to 1 when $\nu \in \mathcal{S}$ and 0 otherwise. It is convenient to define entry-wise Boolean addition and multiplication of characteristic vectors, $\oplus$ and $\circ$, respectively, and also the notation $\mathbf{1}, \mathbf{0}$ to denote the (column) vectors with all 1's and all 0's, respectively. Then, it can be shown that $(\mathcal{A}, \mathcal{B}, \mathcal{C})$ is a 3-partition of $\mathcal{V}$ if and only if

$$\mathrm{I}_{\mathcal{A}} \oplus \mathrm{I}_{\mathcal{B}} \oplus \mathrm{I}_{\mathcal{C}} = \mathbf{1}, \tag{5a}$$

$$\mathrm{I}_{\mathcal{A}} \circ \mathrm{I}_{\mathcal{B}} = \mathrm{I}_{\mathcal{B}} \circ \mathrm{I}_{\mathcal{C}} = \mathrm{I}_{\mathcal{C}} \circ \mathrm{I}_{\mathcal{A}} = \mathbf{0}, \tag{5b}$$

Given F, as before, and a 3-partition $(\mathcal{A}, \mathcal{B}, \mathcal{C})$ of the (ordered) vertex set $\mathcal{V}$, then $\mathrm{I}_{\mathcal{A}}^{\mathsf{T}} \mathsf{F} \mathrm{I}_{\mathcal{B}}$ is the (signed) flux directed from $\mathcal{A}$ to $\mathcal{B}$. That is, if $\mathrm{I}_{\mathcal{A}}^{\mathsf{T}} \mathsf{F} \mathrm{I}_{\mathcal{B}} < 0$, the net flux, summed over all edges connecting directly $\mathcal{A}$ and $\mathcal{B}$, is directed from $\mathcal{B}$ into $\mathcal{A}$. Thus,

$$\mathrm{I}_{\mathcal{A}}^{\mathsf{T}} \mathsf{F} \mathrm{I}_{\mathcal{B}} = -\mathrm{I}_{\mathcal{B}}^{\mathsf{T}} \mathsf{F} \mathrm{I}_{\mathcal{A}},$$

while the absolute value $|\mathrm{I}_{\mathcal{A}}^{\mathsf{T}} \mathsf{F} \mathrm{I}_{\mathcal{B}}|$ is the total net flux between the two parts. In fact, for any 3-partition $(\mathcal{A}, \mathcal{B}, \mathcal{C})$ of the (ordered) vertex set $\mathcal{V}$, it can be shown that

$$\mathrm{I}_{\mathcal{A}}^{\mathsf{T}} \mathsf{F} \mathrm{I}_{\mathcal{B}} = \mathrm{I}_{\mathcal{B}}^{\mathsf{T}} \mathsf{F} \mathrm{I}_{\mathcal{C}} = \mathrm{I}_{\mathcal{C}}^{\mathsf{T}} \mathsf{F} \mathrm{I}_{\mathcal{A}}.$$

Now, one is naturaly led to define the circulation

$$\mathsf{c}(\mathcal{A}, \mathcal{B}, \mathcal{C}) := |\mathrm{I}_{\mathcal{A}}^{\mathsf{T}} \mathsf{F} \mathrm{I}_{\mathcal{B}}|$$

associated to any given 3-partition and, accordingly, the maximal macroscopic circulation

$$\mathsf{c}_{\max} := \max_{\text{3-partitions}} \mathsf{c}(\mathcal{A}, \mathcal{B}, \mathcal{C}).$$

Evidently, $\mathsf{c}(\mathcal{A}, \mathcal{B}, \mathcal{C})$ depends on the partition as well as the "divergence-free" flow field on the graph $\mathcal{G} = (\mathcal{V}, \mathcal{E})$ that is specified by the skew symmetric matrix F (which is implicit in the notation from the context).

A moment's reflection reveals that these concepts do not take into account the topology of the partition. More specifically, the nature and size of the boundary between the parts of a partition may be relevant to the type of global feature one may want to capture. One option is to normalize the flux between any two parts of a partition, by dividing by the size of the corresponding boundaries. However, such an approach leads us to a combinatorial problem with possible number of cases to consider being a Stirling number of the second kind [1] in the number of vertices. Thus, in this paper, we focus on the case of planar graphs, where partitions and a rather natural notion of circulation can be easily computed.

IV. Planar graphs and network circulation

We are interested in the case where geographic proximity of nodes is dictated by an actual embedding of the graph into a linear (metric) space, specifically $\mathbb{R}^2$. Graphs that can be embedded in $\mathbb{R}^2$, without intersection of edges, are called *planar*. Flow fields on such graphs have a resemblance to planar vector fields on manifold. Circulation in vector fields on 2-dimensional manifolds, relates to the curl in a certain canonical decomposition, and can be conveniently quantified by a scalar potential. As we will see, a similar fact holds true for planar graphs, and a notion of circulation can be defined and quantified by a scalar potential on the vertex set of a dual graph. We next discuss planar graphs juxtaposed with elements of Helmholtz-Hodge decomposition of vector fields for insight into the corresponding flow fields on graphs.

A. Planar graphs

Graph planarity is a well studied topic going back to Euler who showed that, for planar graphs,

$$|\mathcal{V}| - |\mathcal{E}| + |\mathcal{F}| = 2, \tag{6}$$

with $\mathcal{F}$ the face set (with the exterior of the graph counted in as an outside face). Interestingly, Euler formula is not sufficient to ensure planarity. A condition that fully characterized planarity was given in 1930's by Kuratowski and Wagner and it is the absence of two specific subgraphs, K_5 or $\mathsf{K}_{3,3}$ [2], [3], [4], [5].

The next important consideration is how to embed a planar graph in $\mathbb{R}^2$, see [6]. It turns out that there may be several "nonequivalent embeddings" [7], [8] and,

moreover, as we will see, network circulation depends on the particular embedding.

Interestingly, every planar graph can be drawn on a sphere (and vice versa) by a sterographic projection. This amounts to projecting points on $\mathbb{R}^2$ onto the (Riemann) sphere corresponding the "north pole" with the "point at ∞." For our purposes, two graph embeddings are said to be *equivalent* if their corresponding projections onto the sphere can be continuously rotated (and the corresponding vertices shifted onto the sphere without crossing edges) so as to match. The equivalence of two graphs is exemplified in Figure 1. In fact, it turns out that there are $m = |\mathcal{F}|$ isomorphic embeddings for every planar graph.

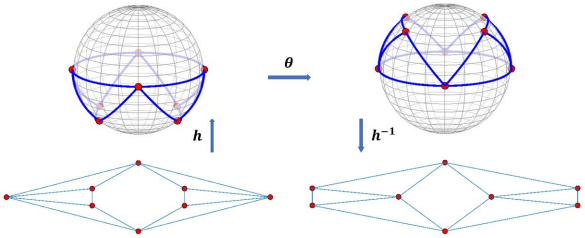

Fig. 1: Isomorphic graphs and sequence of graph morphisms; θ and h are rotation and projection maps, respectively.

B. Helmholtz-Hodge decomposition

The Helmholtz-Hodge decomposition [9], [10], states that the space of vector fields on a manifold can be uniquely decomposed into mutually L^2-orthogonal subspaces using potential functions [11]. These can be expressed as the gradient of a scalar potential, curl of vector potential, and harmonic component that is both "divergence-free" and "curl-free".

In the case of vector fields on $\mathbb{R}^2$, the curl can be expressed as $\Psi = J\nabla\psi$, where J is an antisymmetric matrix and ψ a scalar potential. It can further be shown (Stokes' theorem) that the flux crossing any curve connecting two points a and b on $\mathbb{R}^2$ is given by the difference of the endpoint potentials. It follows that the flux across the path connecting the extrema of a curl potential field is maximum, and this gives us a way to define optimal partitions by spliting the manifold into three parts, that connect the two extreme points of the potential ψ. In a bit more detail, the flux between two points $a, b \in \mathbb{R}^2$ is defined as

$$I = \int_a^b J\nabla\psi \cdot Jds,$$

in which the operator J rotates a 2D vector counterclockwise by $\pi/2$. Then, the flux across any path linking a and b is

$$I = \int_a^b J\nabla\psi \cdot Jds = \int_a^b \nabla\psi \cdot ds = \psi(b) - \psi(a). \tag{7}$$

Hence,

$$\max(I) = \max_{a,b\in\mathbb{R}^2} (\psi(b) - \psi(a)). \tag{8}$$

That is, $\psi(a)$ and $\psi(b)$ are the minimum and maximum curl potentials, respectively. Partitioning the manifold into three regions now can be done by delineating the regions to lie between three (non-intersecting) paths connecting a and b.

C. Planar Graphs

Starting from an antisymmetric net flux matrix $F = [F_{ij}]_{i,j}$ in (2) of Markov chain on a planar graph, we consider the graph with adjacency matrix having the zero pattern of F; the space of vertices and edges are the collection of the nodes and edges, respectively, that have corresponding non-zero elements in F,

$$\mathcal{V}_F = \{v_i \in \mathcal{V} \mid F_{ij} \neq 0\}, \ \mathcal{E}_F = \{e_{ij} \in \mathcal{E} \mid F_{ij} \neq 0\}.$$

In addition we specify a sign function $\sigma : \mathcal{E}_F \times \mathcal{V}_F \to \{-1, 1\}$ that assigns an orientation, specifically $\sigma = \text{sign}(F_{ij})$ for all non-zero elements of the net flux matrix, and define the digraph $\mathcal{G}_F(\mathcal{V}_F, \mathcal{E}_F, \sigma)$. The vector of edge flow weights

$$\mathcal{W} = (w_{ij})_{i,j}$$

corresponding to edges $e_{ij} \in \mathcal{E}_F$ with values $w_{ij} = |F_{ij}|$ represents the flow field. The space of all flow fields is denoted by $\mathcal{U}_F$ and assumes a Helmholtz-Hodge decomposition,

$$\mathcal{U}_F = \mathcal{U}_F^{\text{curl}} \oplus \mathcal{U}_F^{\text{harmonic}} \oplus \mathcal{U}_F^{\text{gradient}},$$

where $\mathcal{U}_F^{\text{gradient}}$ and $\mathcal{U}_F^{\text{curl}}$ are curl-free and divergent-free components. If $\mathcal{W}_{\text{curl}}, \mathcal{W}_{\text{harmonic}}, \mathcal{W}_{\text{gradient}}$ denote projections of $\mathcal{W}$ in the respective components, then clearly $\mathcal{W}_{\text{gradient}} = \mathbf{0}$, since by assumption F has no "sources."

We wish to capture circulation in a similar manner as in planar flow fields and thereby we seek a curl potential ψ. The harmonic component $\mathcal{W}_{\text{harmonic}}$ relates to circulation about "holes" (non-triangular faces [12]) in the graph. Thus, before we proceed, we triangulate $\mathcal{G}_F$, and generate a new graph $\mathcal{G}_F^{\text{chordal}}$, by adding suitably many edges with zero flux (i.e., zeros in the corresponding entries of the flow field, formely $\mathcal{W}$), so as to remove holes and ensure that the harmonic component is zero as well. Thus, we replace the holes with chordal subgraphs by adding the minimum number of chords, that are not part of the cycle but each connects two vertices of the cycle. In this way, we generate a planar chordal graph such that every chordless cycle subgraph is a triangle.

The corresponding potential function ψ is now defined on the graph's faces, and hence, can be assigned to the nodes of the dual graph, $(\mathcal{G}_F^{\text{chordal}})^*$. The maximum flux, in complete analogy with (8), is then obtained by identifying those vertices of the dual graph with minimum and maximum curl potentials.

V. Graph Partitioning

We summarize the insights gained and highlight the steps needed in Algorithm 1 which helps obtain a 3-partition corresponding to maximum circulation by providing the curl potential ψ on the vertices of its dual graph (i.e., faces of the original graph) and how to numerically calculate this. The outcome depends on the embedding of $\mathcal{G}_F$, further discussed in Section VI.

Algorithm 1: Finding curl potential extrema

Input:

A strongly connected, aperiodic, planar, digraph $\mathcal{G}$ with a transition matrix Π.

Offline Preprocessing:

1. Calculate the net flux matrix F from (2).
2. Construct and triangulate $\mathcal{G}_F$ as described in Subsection IV-C, to generate $\mathcal{G}_F^{\text{chordal}}$.
3. Find dual graph $(\mathcal{G}_F^{\text{chordal}})^*$.
4. Set the potential ψ for the outside face to zero.

Computations:

Repeat $(m-1)$ times:

1. Find ψ for vertices of the dual graph using (7) (consider e.g., clockwise as positive direction).

Output:

Two faces of the primal with potential extrema.

Knowing ψ allows carving 3-partitions that entail maximal circulation. Indeed, any set of two paths on the dual graph between the points of ψ-extrema separates the graph in the three regions, A, B and C, discussed earlier. This is summarized next.

Proposition 2. *Consider a divergence-free flow field $\mathcal{W}$ on the edges of a strongly connected digraph. Algorithm 1 generates the chordal digraph $\mathcal{G}_F^{\text{chordal}}$ and its dual with an associated curl potential ψ. Then, there exist paths in the dual graph connecting two chosen extrema points of ψ that provide a 3-partition with maximal macroscopic circulation.*

Proof. Completion of the graph into a chordal graph is the first step of the algorithm and was explained before. We compute ψ as follows. We assign 0 at the vertex of the dual of the chordal graph corresponding to the outside face, and proceed to assign values to the remaining vertices of the dual graph so that the difference between values of adjacent vertices equals the (signed, e.g., in the clockwise sense) flux on the corresponding edge of the primal graph. We now explain the last part of the proposition.

Since $\mathcal{G}_F^{\text{chordal}}$ is simple, its dual is 3-edge-connected. By Menger theorem [13], [14], for 3-edge-connected graphs every pair of vertices has 3 edge-disjoint paths in between. Now consider a pair of vertices on the dual graph corresponding to a minimum and maximum of ψ. The connecting 3 edge-disjoint paths, P_1, P_2, and P_3 generate three cycles, C_1, C_2, and C_3, e.g., $P_2 \cup P_1 = C_1$, $P_2 \cup P_3 = C_2$, and $P_1 \cup P_3 = C_3$. If the extrema of the scalar potential do not include the outside node of the (now chordal) dual graph, which is the only node with degree higher than three, two paths may share this node as well as the extremal nodes. As a consequence, the outside will be visited twice while tracing C_i. Properly selecting interior or exterior of those cycles, these delineate three disjoint sets of primal vertices. Then, that by (8), the flow that crosses their shared boundaries (i.e., P_1, P_2, and P_3) is maximal. □

Fig. 3 exemplifies the result of Proposition 2 for a planar graph with two non-equivalent embeddings, where the 3-partitions are marked using different colors (red, blue, green) and shapes (□, ○, △). We note that for a planar, strongly connected graph, provided the "outside" is not a part of the path between extremum potentials in the dual, the partitions are connected. This follows from the fact that the graph is chordal.

VI. Effect of Embedding on Graph Partitioning

Whitney showed that 3-connected graphs have unique embedding, and consequently unique dual graph [7]. But in general it is possible that if we consider two different embeddings $\mathcal{G}_1, \mathcal{G}_2$ of a planar graph $\mathcal{G}$, the duals $\mathcal{G}_1^*, \mathcal{G}_2^*$ become non-isomorphic. And this may result into a different output in Algorithm 1.

A. Example

Given transition matrix for a planar graph as in (9), netflux matrix is calculated using equation (2). Fig. 2 indicates two possible graphs which are constructed based on calculated net flux matrix. These two embeddings of a connected planar graph are related by flipping at separating pair. As described in IV-C, graphs are triangulated, $\mathcal{G}_1', \mathcal{G}_2'$ in Fig. 3.

$$\Pi = \begin{bmatrix} 0 & 0.25 & 0 & 0 & 0.25 & 0 & 0.25 & 0.25 \\ 0.333 & 0 & 0.333 & 0.333 & 0 & 0 & 0 & 0 \\ 0 & 0.25 & 0 & 0.25 & 0 & 0.25 & 0 & 0.25 \\ 0 & 0.333 & 0.333 & 0 & 0.333 & 0 & 0 & 0 \\ 0.333 & 0.333 & 0 & 0.333 & 0 & 0 & 0 & 0 \\ 0 & 0 & 0.333 & 0 & 0 & 0 & 0.333 & 0.333 \\ 0.5 & 0 & 0 & 0 & 0 & 0.5 & 0 & 0 \\ 0.25 & 0 & 0.25 & 0 & 0 & 0.25 & 0.25 & 0 \end{bmatrix} \tag{9}$$

Fig. 2: Two possible embeddings, constructed based on netflux matrix.

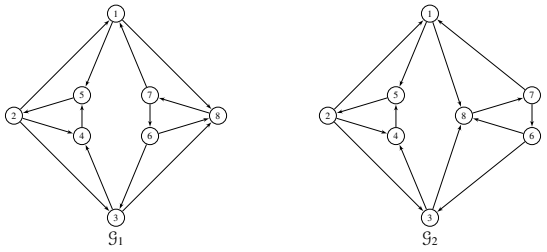

Fig. 3: Triangulated and dual of the graphs in Fig. 2 and their 3-partitions.

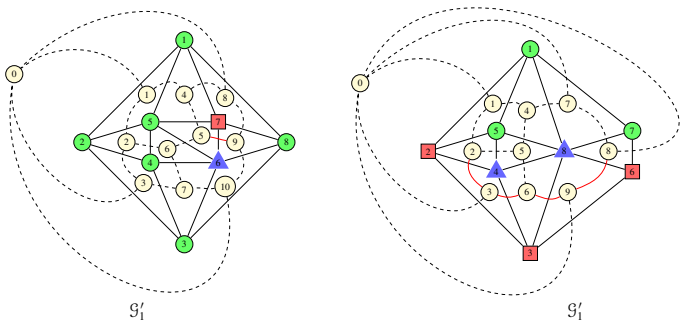

Based on the Algorithm 1, vector of curl potentials for each triangulated graph is calculated,

$$\begin{aligned}\psi_1&=[0,-0.0076,0.0181,0.0082,0.0064,0.0064,0.0064,0.0064,0.009,0.0205,-0.0096]^{\mathrm{T}},\\ \psi_2&=[0,-0.0076,0.0181,0.0082,0.0064,0.0064,0.0064,-0.0025,-0.014,0.016]^{\mathrm{T}}.\end{aligned} \tag{10}$$

where ψ_{i_j} corresponds to the curl potential of the j^{th} face of graph $\mathcal{G}'_i$, $i \in \{1,2\}$.

The faces with maximum and minimum potential for $\mathcal{G}'_1$ and $\mathcal{G}'_2$ are $\{5,9\}$ and $\{2,8\}$, respectively. Applying Proposition 2, the 3-partitions for them are $\{\{6\},\{7\},\{1,2,3,4,5,8\}\}$ and $\{\{4,8\},\{2,3,6\},\{1,5,7\}\}$, respectively.

This example highlights that the output of Algorithm 1, and consequently the partitioning of a graph, varies according to the particular embedding chosen.

REFERENCES

[1] J. Quaintance, *Combinatorial Identities for Stirling Numbers: The Unpublished Notes of H W Gould*. World Scientific, 2015.

[2] S. Sarvottamananda, "Lecture notes in planar graphs, planarity testing and embedding," October 2014.

[3] K. Kuratowski, "Sur le problème des courbes gauches en topologie," *Fundamenta Mathematicae*, vol. 15, no. 1, pp. 271–283, 1930. [Online]. Available: http://eudml.org/doc/212352

[4] K. Wagner, "Uber eine Erweiterung eines Satzes von Kuratowski," *Deutsche Mathematik*, vol. 2, pp. 280–285, 1937.

[5] C. Thomassen, "Planarity and duality of finite and infinite graphs," *Journal of Combinatorial Theory, Series B*, vol. 29, no. 2, pp. 244–271, 1980.

[6] G. Nemhauser and L. Wolsey, "Integer programming and combinatorial optimization," in *Wiley, 1988*. Springer, 1999.

[7] H. Whitney, "Congruent graphs and the connectivity of graphs," in *H. Whitney Collected Papers*. Springer, 1992, pp. 61–79.

[8] A. Gagarin, W. Kocay, and D. Neilson, "Embeddings of small graphs on the torus," *Cubo Mat. Edu.*, vol. 5, 2003.

[9] H. Helmholtz, "Uber integrale der Hydrodynamischen Gleichungen, Welche den Wirbelbewegungen Entsprechen," *Journal fur die reine und angewandte Mathematik*, vol. 1858, no. 55, pp. 25–55, January 1858.

[10] W. V. D. Hodge, *The theory and applications of harmonic integrals*. Cambridge University Press, 1941.

[11] H. Bhatia, G. Norgard, V. Pascucci, and P.-T. Bremer, "The Helmholtz-Hodge decomposition-a survey," *IEEE Transactions on Visualization and Computer Graphics*, vol. 19, no. 8, pp. 1386–1404, 2012.

[12] L. Lim, "Hodge laplacians on graphs," *CoRR*, 2015. [Online]. Available: http://arxiv.org/abs/1507.05379

[13] K. Menger, "Zur allgemeinen kurventheorie," *Fundamenta Mathematicae*, vol. 10, no. 1, pp. 96–115, 1927.

[14] C. Doczkal, "Short proof of Menger's theorem in coq (proof pearl)," *HAL-02086931*, 2019.